JOURNAL OF APPLIED ELECTROCHEMISTRY **28** (1998) 1195–1203

Influence of Co^{2+} ions on cathode behaviour during zinc electrowinning

T. DOBREV

Institute of Physical Chemistry, Bulgarian Academy of Sciences, 1113 SOFIA, Bulgaria

C. CACHET, R. WIART*

UPR 15 CNRS Physique des Liquides et Électrochimie, Université Pierre et Marie Curie, Tour 22, 4 Place Jussieu, 75252 Paris, Cedex 05, France

Received 27 January 1998; accepted in revised form 27 May 1998

The effect of Co^{2+} ions on zinc deposition from acidic sulfate electrolytes is investigated on the basis of steady-state polarization curves and impedance measurements. Hydrogen evolution is shown to be enhanced by adsorbed cobalt on both the zinc deposit and the aluminium substrate, and this stimulation occurs in combination with the catalytic effect of adsorbed species originating from anodic products. Hydrogen evolution involves a diffusion-controlled step and a slow adsorption process which is the rate-determining step. It also induces the redissolution of the zinc deposit observable from the potential dependencies of current, charge transfer resistance and double layer capacitance.

Keywords: *zinc deposition*, *acid sulfate electrolyte*, *Co^{2+} ions*, *hydrogen evolution*

1. Introduction

The zinc electrowinning industry is faced with the problem of obtaining a zinc deposit free of metal impurities. Thorough purification of the solution is necessary because almost all metal impurities, except for manganese, are more noble than zinc. Thus they are deposited either before, or simultaneously with zinc, forming galvanic cells on the cathode surface leading to the redissolution of zinc in the acidic electrolyte. Thus such codeposited impurities markedly decrease the current efficiency of zinc electrowinning. Moreover the combined effect of these impurities is not simply additive, but catalytic.

To explain the effect of these impurities, many basic investigations have been reported, mainly in terms of current efficiency, cyclic voltammetry, morphology and deposit orientation [1–8]. Zinc deposition is affected by bath acidity, temperature, current density, the nature and concentration of impurities and substrates. Zinc electrowinning in highly acidic sulphate electrolytes containing cobalt or nickel as impurity shows an 'induction period' before the redissolution of the zinc deposit [4, 9–12]. The length of the induction period decreases with increasing temperature, increasing acid concentration and with decreasing current density [1, 3, 12]. It has been shown [1] that the deleterious effect of impurities on current efficiency of zinc deposition follows the order Ge > Sb > Ni > Co > Bi > Cu > As > Sn.

From cyclic voltammetry, the impurities such as Ge, Ni and Co have been found to produce one, or several, characteristic hydrogen peaks, the height of which was shown to increase with the impurity concentration in the solution [13]. Zinc deposition polarization curves were more sensitive to nickel than to cobalt in the electrolyte [14]. A 'synergism' effect of impurities on zinc electrowinning has been reported for electrolytes containing admixtures of Ni^{2+} and Co^{2+} [15]. This effect was ascribed to the specific adsorption of cobalt complexes $(Co(SO_4)_n)^{(2n-2)-}$ which catalyses the partial rate of nickel codeposition with zinc.

Recently, on the basis of steady-state polarization curves and electrochemical impedance analysis, new data on the effect of metal impurities on zinc deposition have been reported [10, 11, 16–20]. The influence of Ni^{2+} ions [17] on the kinetics of electrodeposition has been interpreted in terms of a reaction model involving hydrogen adsorption and evolution, a multistep mechanism for zinc deposition and the overall reaction for zinc dissolution. The presence of Ni^{2+} in the electrolyte interferes with anodically formed species to favour the formation of active sites for hydrogen evolution and thereby destabilize the deposition conditions and trigger deposit corrosion [17]. Then the slow accumulation of adsorbed nickel results in a progressive reduction of the current domain in which zinc deposition is predominant. In the presence of Ge^{4+} ions, zinc deposition is superseded by hydrogen evolution whose kinetics have been shown to be entirely controlled by two distinct germanium species adsorbed on the zinc

* Author to whom correspondence should be sent.

0021-891X

electrode [20]. On the other hand, lead adsorption has been shown to decrease specifically the rate constants of zinc dissolution and hydrogen evolution [19].

In the present work, the effect of Co^{2+} ions on zinc deposition from acidic sulfate electrolytes used for zinc electrowinning is investigated on the basis of steady-state polarization curves and impedance measurements, with a view to obtaining new information on the mechanism of zinc deposition in the presence of these ions.

2. Experimental details

Experimental details have been described previously [11]. The electrolysis cell was thermostated at (37 ± 1) °C. The cathode of 1 cm^2 surface area was made of aluminium used in zinc electrowinning industry (Union Minière); the substrate purity is indicated in Table 1. The cathode surface was vertically oriented in the cell, and defined with epoxide resin (Buehler). Before electrolysis, the cathode surface was polished with emery paper (grit 1200). The reference electrode consisted of mercury/mercurous sulphate electrode in saturated potassium sulphate (SSE), used with two compartments separated by fritted glass. The counter electrode was a platinum gauze cylinder. The base electrolyte was made of 55 g dm^{-3} zinc from $ZnSO_4.7\,H_2O$ and 120 g dm^{-3} H_2SO_4 in pure water, which was doubly ion-exchanged and twice distilled in a quartz apparatus. Co^{2+} ions were added to the electrolyte from a $CoSO_4.7\,H_2O$ solution in pure water. All chemicals were Merck products of analytical grade purity and the maximum levels of impurities in the electrolyte were: Ca, K, Li, Mg, Na, Pb 2 ppm; Cd, Cu, Fe, Sr 1 ppm; Mn O.6 ppm; As 0.1 ppm.

Steady-state polarization curves and impedance measurements in the frequency range from 60 kHz to 6 mHz were performed automatically using a frequency response analyser (Solartron SI 1250) and an electrochemical interface (Solartron SI 1286) controlled by a microcomputer (IBM PS/2 model 35 slc) with Software (Fracom).

Before starting each potentiostatic curve, the electrode was maintained at the initial potential for a prepolarization time τ_p (between 5 min and 1 h). Potentiostatic curves were obtained by potential steps of 10 mV from $U = -1.56$ V down to −1.4 V, or from $U = -1.3$ V up to −1.7 V, and waiting for current stabilization for 15 min at each potential U before measuring the electrode impedance. Generally this current stabilization, equivalent to a variation lower than 2%, occurred in spite of the time dependences of the morphology and roughness of zinc deposits. The high-frequency limit of electrode impedance yields the electrolyte resistance, R_e, which was used to correct the ohmic drop, $R_e i$, in the steady-state polarization curves i/E, with $E = U - R_e i$ where negative values of current density, i, correspond to the cathodic current. With such an experimental procedure, the total time necessary for one experiment was approximately 15 h.

Surface examination of the cathode was performed by SEM and X-ray EDS.

3. Results and discussion

To determine the interactions between the cobalt species adsorbed on both the zinc deposit and the aluminium substrate, two different procedures were adopted to obtain the polarization curves and impedance spectra. The first consisted in decreasing cathode polarization subsequently to a zinc predeposit obtained at relatively high cathodic polarization. The second was realized by increasing the cathode polarization starting from the aluminium substrate polarized in the domain of hydrogen evolution at relatively low polarization.

3.1. *Decreasing polarization of the electrode*

Steady-state polarization curves of zinc deposition were recorded under potentiostatic conditions from $U = -1.56$ V down to −1.4 V and they were corrected for ohmic drop. Figure 1 shows the influence

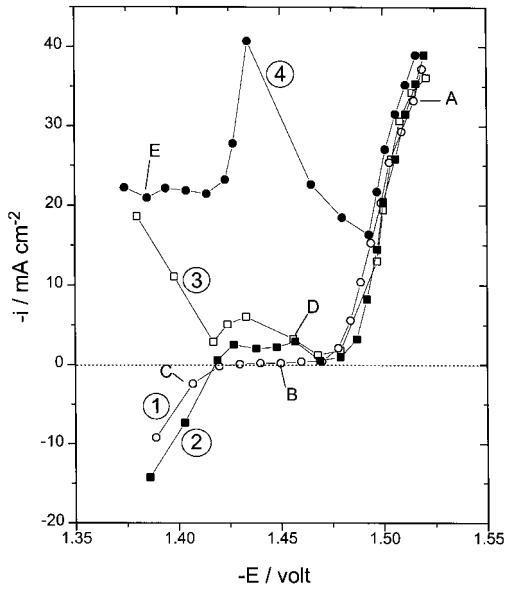

Fig. 1. Steady-state polarization curves $i(E)$ obtained from $U = -1.56$ to −1.4 V vs SSE, for various concentrations [Co^{2+}] in fresh electrolytes: 0 (curve 1), 5 (curve 2), 30 (curve 3) and 100 mg dm^{-3} (curve 4). Polarization time τ_p at $U = -1.56$ V is 5 min. Points: (A) $E = -1.515$ V on curve 1; (B) $E = -1.45$ V on curve 1; (C) $E = -1.41$ V on curve 1; (D) $E = -1.455$ V on curve 3; (E) $E = -1.385$ V on curve 4.

Table 1. Impurity contents in the aluminium substrate

Element	Cu	Si	Ni	Mg	Fe	Zn	B	Ti
Percentage impurity	0.005	0.015	0.0025	0.005	0.35	0.03	0.006	< 0.03

of the concentration of Co^{2+} ions in fresh electrolytes, when the electrode was prepolarized for 5 min at $U = -1.56$ V. As already reported [18] three distinct domains appear on curve 1 obtained without Co^{2+} in the electrolyte, a current plateau (between -1.42 and -1.48 V) separating the cathodic branch for zinc deposition from the anodic branch for zinc dissolution. In addition to the inhibition of zinc deposition by adsorbed hydrogen, the adsorption of lead present in the electrolyte probably contributes to the existence of the current plateau, as previously shown [19]. With increasing Co^{2+} concentration, hydrogen evolution is stimulated and the current plateau is progressively replaced by a current peak. In addition the potential range for hydrogen evolution widens on curve 4 obtained with the highest concentration of Co^{2+}. The current observed between -1.37 and -1.42 V on curves 3 and 4 characterizes hydrogen evolution on the substrate. This current, sensitive to the presence of impurities in the substrate, was observed to be much lower on pure aluminium (99.999% purity, Johnson-Matthey, specpure). On the other hand, it is worth noting that the cathodic branch for zinc deposition is little affected by the presence of Co^{2+}: only a slight increase in the current appears on curve 4 between -1.49 and -1.52 V.

The impedance plots characteristic of the three domains on curve 1 in Fig. 1 are depicted in Fig. 2.

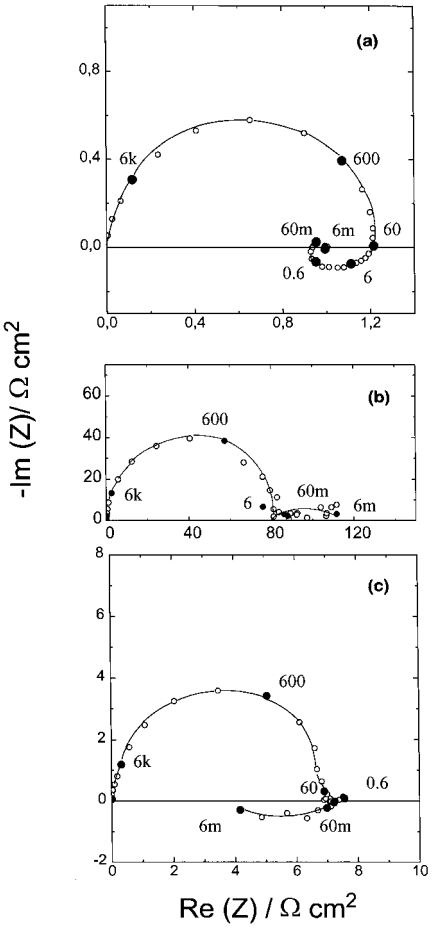

Fig. 2. Complex plane impedance plots (a, b, c) obtained at points A, B and C, respectively, in Fig. 1, without Co^{2+} with electrolyte.

Figure 2(a) shows the general features for zinc deposition: a high-frequency capacitive loop due to the charge transfer resistance of zinc deposition in parallel with the double layer capacitance, an inductive feature with two distinct time constants (at 6 and 0.6 Hz, approximately) and a low frequency capacitive loop, as already reported [18, 19]. The relaxation processes apparent in the faradaic impedance have been interpreted in terms of a reaction model where hydrogen adsorption is coupled to the multi-step mechanism for zinc deposition [17, 19].

Figure 2(b) is typical of the current plateau where a small amount of hydrogen evolution takes place on the zinc deposit: this plot essentially exhibits a charge transfer loop accompanied by a small low-frequency capacitive loop, indicating that some inhibiting adsorption is involved in hydrogen evolution.

Figure 2(c) corresponds to the dissolution of the zinc deposit ($i > 0$): a small capacitive loop and an inductive loop appear in the low-frequency domain.

The presence of Co^{2+} in the electrolyte does not change the shape of the impedance plots characteristic of zinc deposition, even between -1.49 and -1.52 V on curve 4. At potentials where the formation of hydrogen bubbles on the electrode surface predominates, the electrode impedance is difficult to measure accurately in the low-frequency domain. However, when the current was relatively low, significant and typical impedance plots were obtained, as exemplified in Fig. 3. In addition to the charge transfer loop, plot (d) exhibits a low-frequency capacitive loop associated with a negative resistance, in

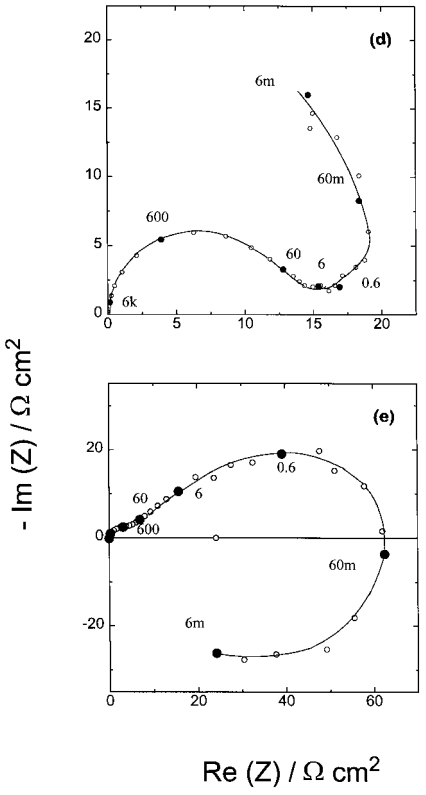

Fig. 3. Complex plane impedance plots (d, e) obtained at points D and E, respectively, in Fig. 1, with Co^{2+} in the electrolyte.

agreement with the negative slope of curve 3 in Fig. 1. This negative slope corresponds to strong inhibition of hydrogen evolution by some adsorbed species. Consequently, it can be considered that the catalytic effect of the adsorbed, or codeposited, Co atoms on hydrogen evolution is strongly reduced by another adsorbate in the potential domain where the negative resistance appears. This counteraction is probably due to the adsorbed zinc species (adatoms or adions) present on the electrode surface [17].

Plot (e) is probably characteristic of hydrogen evolution on the aluminium substrate, after dissolution of the zinc deposit, in the presence of adsorbed, or deposited, cobalt species. Similar to the situation already observed with the Ge impurity [18, 19], a diffusion-type loop at medium frequencies (100–0.4 Hz) and a low frequency inductive loop appear on plot (e). Therefore two distinct adsorbates are probably involved in the mechanism of hydrogen evolution: one whose surface concentration is diffusion controlled, acting as an inhibitor, and a second producing a slow catalytic effect. On plot (d), the Warburg-type behaviour is barely apparent at frequencies between 6 and 0.15 Hz.

The dependence of the product of the charge transfer resistance, R_t, and current density, i, on the electrode potential, E, is illustrated in Fig. 4. In the cathodic domain (−1.48 to −1.52 V) the variation of $R_t i$ corresponds to zinc deposition and is not affected by the presence of 5 mg dm^{-3} Co^{2+} in the electrolyte. In the potential domain (−1.42 to −1.48 V), curves 1, 2 and 3 show a peak characteristic of hydrogen evolution, in agreement with previously reported results on the influence of Ni^{2+} or Ge^{4+} impurities [11, 16–19]. Figure 4 shows that this peak is higher with increasing Co^{2+} concentration. It is also clear from curve 3 that hydrogen evolution influences zinc deposition at potentials less cathodic than −1.5 V. On curve 4 corresponding to 100 mg dm^{-3} Co^{2+}, hydrogen evolution remains prevalent at low cathodic polarization and the $R_t i$ product remains relatively high.

The values of the double layer capacitance, C_d, deduced from the apex of the high frequency loop on the impedance plots, are given in Fig. 5, the experimental conditions being the same as for Fig. 4. With decreasing cathodic potential E from −1.52 V, the capacitance decreases as the deposition current progressively vanishes. This decrease is connected with an increasing quantity of adsorbed hydrogen on the zinc electrode. At low cathodic polarizations ($E > -1.42$ V), the increase in C_d indicates an increase in the electrode area due to the dissolution of the zinc deposit. This effect is more pronounced on curves 2 and 3 corresponding to 5 and 30 mg dm^{-3} Co^{2+}, respectively. On curve 3 the observed C_d peak shows that the deposit disappears on the electrode surface. For 100 mg dm^{-3} Co^{2+}, the dissolution of the zinc deposit occurs at more cathodic potentials, and the low values of C_d observed at low cathodic polarizations characterize the hydrogen adsorption on the substrate.

The hydrogen evolution current depends not only on [Co^{2+}], but also on the electrolyte ageing, as illustrated in Fig. 6: the hydrogen peak is higher on curve 3 than on curve 2. In addition, it appears from curve 3 that the dissolution of the zinc deposit occurs suddenly with the aged electrolyte: when the electrode potential E attains a critical value (−1.42 V) with decreasing cathodic polarization, a sharp decrease in cathodic current is observed. As shown in Fig. 7, this current decrease is simultaneous with both a sharp increase in $R_t i$ and the presence of an acute peak of C_d. After complete dissolution of the deposit ($E > -1.42$ V), $R_t i$ remains high, and C_d remains low, due to the hydrogen evolution taking place on the aluminium substrate and stimulated by the adsorption or deposition of cobalt.

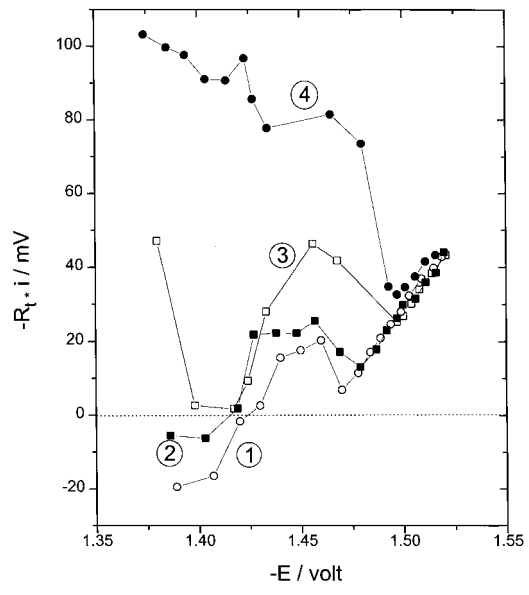

Fig. 4. Potential dependence of the $R_t i$ product under the same conditions as for Fig. 1. Concentration of Co^{2+}: 0 (curve 1), 5 (curve 2), 30 (curve 3) and 100 mg dm^{-3} (curve 4).

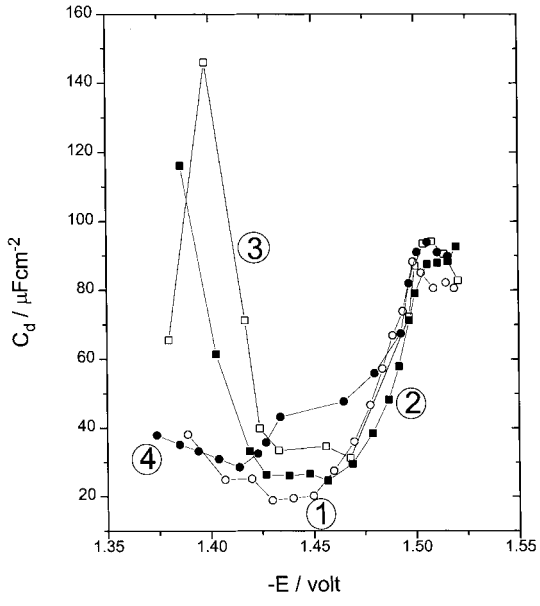

Fig. 5. Potential dependence of the double layer capacitance under the same conditions as for Fig. 1. Concentration of Co^{2+}: 0 (curve 1), 5 (curve 2), 30 (curve 3) and 100 mg dm^{-3} (curve 4).

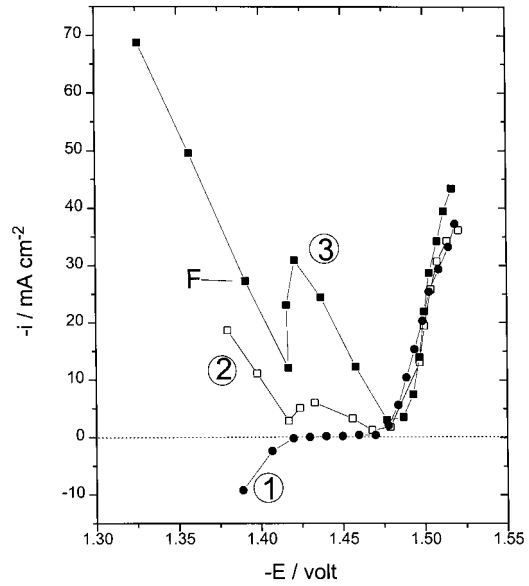

Fig. 6. Influence of the electrolyte ageing on polarization curves $i(E)$ obtained under the same conditions as for Fig. 1: without Co^{2+} (curve 1) and with 30 mg dm^{-3} Co^{2+} in a fresh electrolyte (curve 2) and in an electrolyte aged for 100 h (curve 3). Point F: $E = -1.39$ V.

In the potential domain where hydrogen evolves on the aluminium substrate, the current stability is considerably diminished, and it becomes impossible to obtain significant values of the electrode impedance at frequencies down to 6 mHz. Plot (f) in Fig. 8 is typical of hydrogen evolution on the substrate covered with adsorbed cobalt. Similar to plot (d) in Fig. 3, plot (f) reveals a diffusion-type capacitive feature, and the low-frequency data agree with the negative slope of the polarization curve. However, the origin of the negative resistance is probably different, due to a much less probable adsorption of zinc species in the potential region around point F.

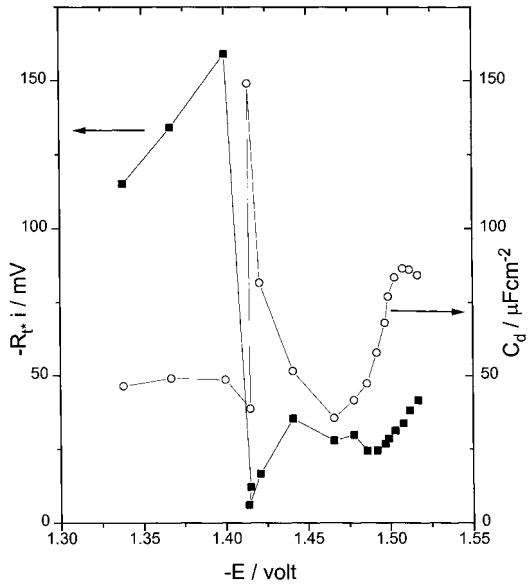

Fig. 7. Potential dependences of the double layer capacitance C_d and the product $R_t i$ under the same conditions as for curve 3 in Fig. 6: $[Co^{2+}] = 30$ mg dm^{-3} and aged electrolyte.

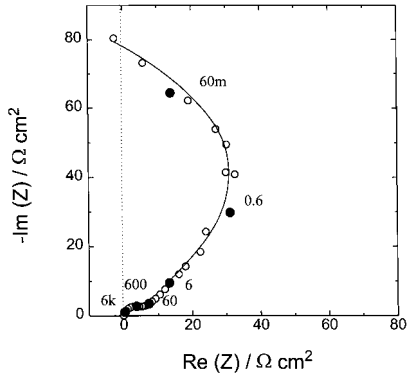

Fig. 8. Complex plane impedance plot obtained at point F in Fig. 6, with Co^{2+} in the aged electrolyte.

Similar concomitant and steep variations in $R_t i$, C_d and i were observed in aged electrolytes for various concentrations $[Co^{2+}]$, but the critical value of the potential E depends on $[Co^{2+}]$: -1.43 V for $[Co^{2+}] = 50$ mg dm^{-3}, -1.42 V for $[Co^{2+}] = 30$ mg dm^{-3}, and -1.41 V for $[Co^{2+}] = 20$ mg dm^{-3}. These values are in agreement with a more stimulated process of zinc redissolution in more concentrated Co^{2+} solution.

The influence of the electrolyte ageing indicates that the stimulation of hydrogen evolution by Co^{2+} ions occurs in combination with the catalytic effect of anodically formed products, as already observed for the impurity Ni [11, 17]. During electrolysis, the progressive accumulation of the adsorbed metal impurity with adsorbed species originating from the anodic products slowly stimulates the hydrogen evolution on the zinc electrode. The minimum current i_m, observed in Figs 1 and 6 at potentials close to -1.48 V and separating the deposition branch from the hydrogen domain, increases with both the concentration $[Co^{2+}]$ in the electrolyte and the electrolysis time.

Under similar experimental conditions, the decrease in the polarization for zinc deposition observed in this study concerning the Co^{2+} impurity, is much lower than that previously reported [16, 17] for the Ni^{2+} impurity present at relatively low concentration (5 mg dm^{-3}). Furthermore the hydrogen peak was markedly higher for Ni^{2+} than for Co^{2+}. Consequently, it can be concluded that the propensity of the metal impurity in the electrolyte to destabilize the conditions for zinc deposition is less marked for Co^{2+} than for Ni^{2+}, in conformity with already reported data [14].

3.2. *Increasing polarization of the electrode*

To obtain further information concerning the influence of Co^{2+} ions on the electrode behaviour at low cathodic polarizations, the aluminium electrode was prepolarized at $U = -1.3$ V and then U was stepped from -1.3 V up to -1.7 V. Figure 9 presents the curves obtained without Co^{2+} (curves 1) and with 100 mg dm^{-3} Co^{2+} (curves 2) in the aged electrolyte for about 100 h. The influence of the ohmic drop

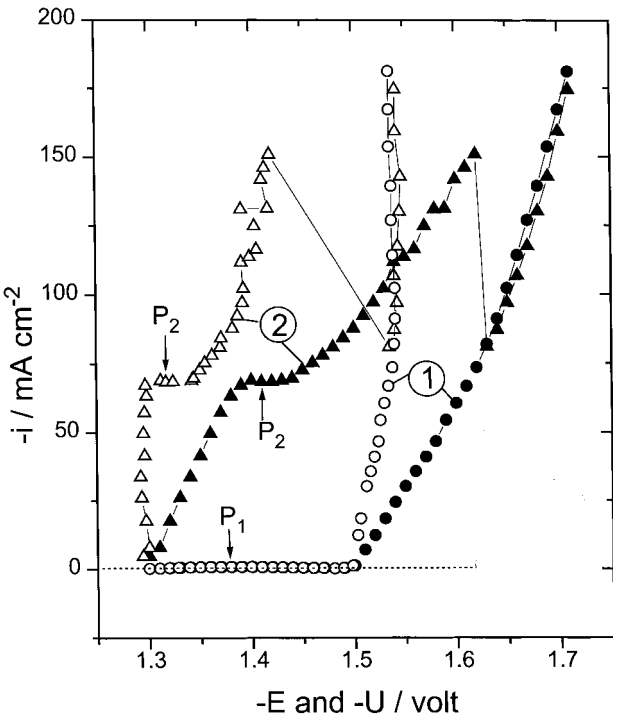

Fig. 9. Polarization curves: (○) i_1 (E), (△) i_2 (E) and (●) i_1 (U), (▲) i_2 (U) obtained from $U = -1.3$ to -1.7 V vs SSE, without Co^{2+} (curves 1) and with 100 mg dm^{-3} Co^{2+} (curves 2) in aged electrolyte. Prepolarization time at $U = -1.3$ V is 30 min.

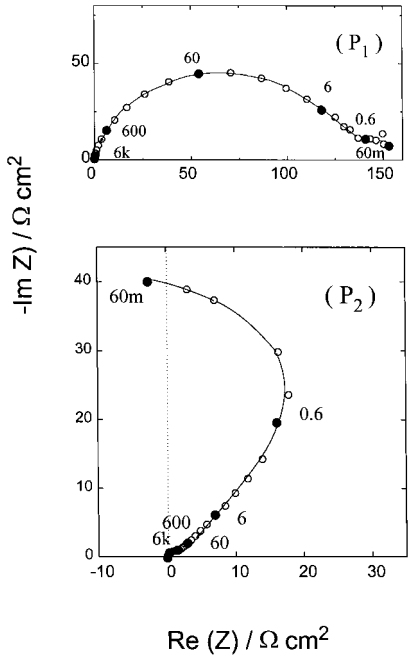

Fig. 10. Complex plane impedance plots obtained at points P_1 and P_2 in Fig. 9. (P_1) $U = -1.38$ V; (P_2) $U = -1.41$ V and $E = -1.325$ V.

appears from a comparison of the $i(U)$ curves with the $i(E)$ curves. The ohmic drop corresponds to a resistance R_e ranging between 0.9 and 1.3 Ω cm^2. This resistance agrees with the highly conducting electrolyte, but it is also affected by the distance between the working electrode and the reference electrode, which was relatively high in the present study.

Without Co^{2+}, there is practically no current up to -1.5 V, a potential where zinc deposition starts. Plot (P_1) in Fig. 10, corresponding to P_1 in Fig. 9, is very similar to Figure 2(b), indicating that hydrogen evolution on the aluminium substrate occurs in the same manner as hydrogen evolution on the zinc deposit.

With the presence of 100 mg dm^{-3} Co^{2+} in the aged electrolyte, hydrogen evolution on the aluminium substrate is considerably stimulated (curves 2 in Fig. 9). Firstly, a sharp increase of current takes place for $E = -1.3$ V. Then a current plateau appears, followed by a new increase in current. Finally, the current decreases suddenly to rejoin the cathodic branch of zinc deposition. In the whole potential domain where hydrogen evolution predominates, a Warburg-type capacitive loop leading to a negative resistance was apparent on impedance plots, as exemplified on plot P_2 in Fig. 10, obtained for $U = -1.41$ V (i.e., $E = -1.325$ V). But the evolution of bubbles and the poor stability of current did not allow significant measurements below 60 mHz and the low-frequency extrapolation was not possible. In the frequency domain (60–0.6 Hz), the Warburg-type impedance on plot P_2 is similar to plots (d), (e) and (f). Therefore it is confirmed that hydrogen evolution on adsorbed cobalt involves a diffusion-controlled process whatever the electrode: zinc deposit or aluminium substrate.

The low-frequency part on plot P_2 is the same as on plot (f), but differs from plot (e) which was obtained with a fresh electrolyte. Consequently, the negative resistance can be related to a stronger inhibition of hydrogen evolution on aluminium in aged electrolyte. This result confirms that the stimulation of hydrogen evolution on the aluminium substrate results from the coupled adsorption of Co species with other species formed during the electrolysis.

In an attempt to clarify the nature of the species present on the electrode surface, various aluminium electrodes were maintained for several hours at a constant potential $U = -1.4$ V, without or with Co^{2+} ions in the electrolyte. The current transients are exemplified in Fig. 11. Curve 1 shows that the long term experiment in the absence of Co^{2+} gives rise to a slow increase in hydrogen current, which might be due to the accumulation of anodic products adsorbed on the aluminium surface and liable to stimulate the hydrogen evolution. Curve 1 also shows a current decrease at the end of the transient, indicating a slow inhibition process. Curve 2 reveals that i increases more rapidly, due to the catalytic effect of Co^{2+} ions on hydrogen evolution. The increase in current during the first hours on curve 2 in Fig. 11 indicates that the curves 2 in Fig. 9 were not really steady-state since there was probably a slow accumulation of adsorbed species, essentially cobalt, able to stimulate the hydrogen evolution.

At the end of the transients in Fig. 11, the examination of electrodes in SEM and X-ray EDS reveals

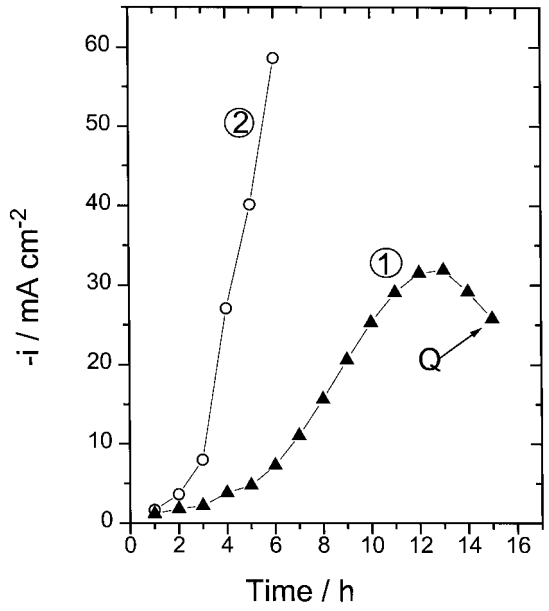

Fig. 11. Time dependence of the current i for an electrode polarized directly at $U = -1.4$ V, without Co^{2+} (curve 1) and with 100 mg dm^{-3} Co^{2+} (curve 2).

the presence of some substrate impurities (Fe and Cu), but also of lead in a few spots on the electrodes, as exemplified in Fig. 12. This indicates the likely inhibition of hydrogen evolution due to lead present on the aluminium surface. In addition, at the end of curve 2 in Fig. 11, the examination of electrodes did not reveal the presence of Co atoms, whose quantity is probably too small on the surface to be detected by this technique.

The potential dependence of the $R_t i$ product, measured under the same conditions as for Fig. 9, is represented in Fig. 13. A clear distinction can be made between the high values of $R_t i$ corresponding to hydrogen evolution and the low values corresponding to zinc deposition which tend towards about 50 mV at the highest cathode polarizations. The two jumps observed at $U = -1.5$ V and $U = -1.62$ V on curves 1 and 2, respectively, correspond to the potentials where zinc deposition starts on Fig. 9.

The influence of the direction for potential stepping is depicted in Fig. 14. The coincidence of curves appears for hydrogen evolution on the left hand side of the figure and for zinc deposition on the right hand side. In addition, the transition between the two regimes appears to take place at the same potential $E = -1.43$ V, whatever the direction of the potential stepping. The aluminium electrode exists on the left hand side whereas a zinc deposit exists on the right hand side. It appears that the curve for hydrogen evolution on the aluminium substrate depends on the direction of potential stepping, due to the influence of the electrode story.

4. Conclusion

Steady-state polarization curves and impedance data show that the kinetics of zinc deposition taking place at high cathodic potentials are little affected by the presence of Co^{2+} ions in the electrolyte. However with Co^{2+} ions, a current peak of hydrogen evolution on zinc deposit appears at low cathodic potentials, and the peak height increases with [Co^{2+}] concentration.

Impedance spectra characteristic of hydrogen evolution reveal that the mechanism of hydrogen evolution due to the adsorbed cobalt involves a diffusion-controlled process.

In addition, the rate determining step of hydrogen evolution is a slow adsorption process able to give rise to a capacitive feature when the polarization resistance is negative. Such a negative resistance probably results from a strong inhibition of hydrogen evolution by adsorbed zinc species.

From impedance data in the high frequency domain, it is shown that hydrogen evolution on ad-

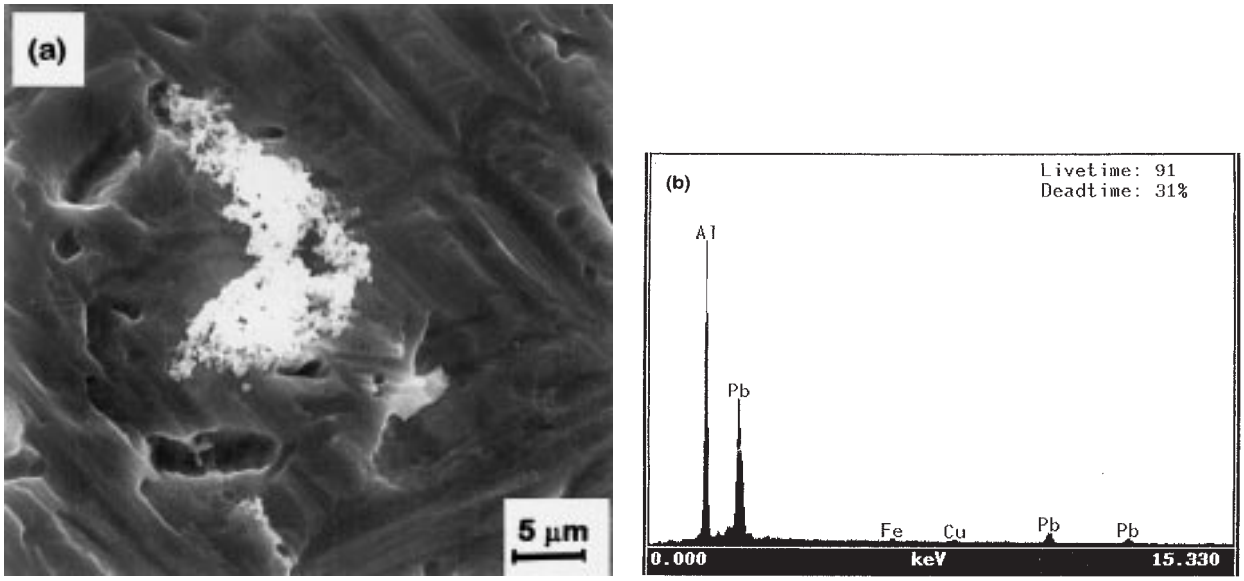

Fig. 12. (a) SEM of the electrode obtained at point Q in Fig. 11. (b) X-Ray EDS analysis of the spot in Fig. 12(a).

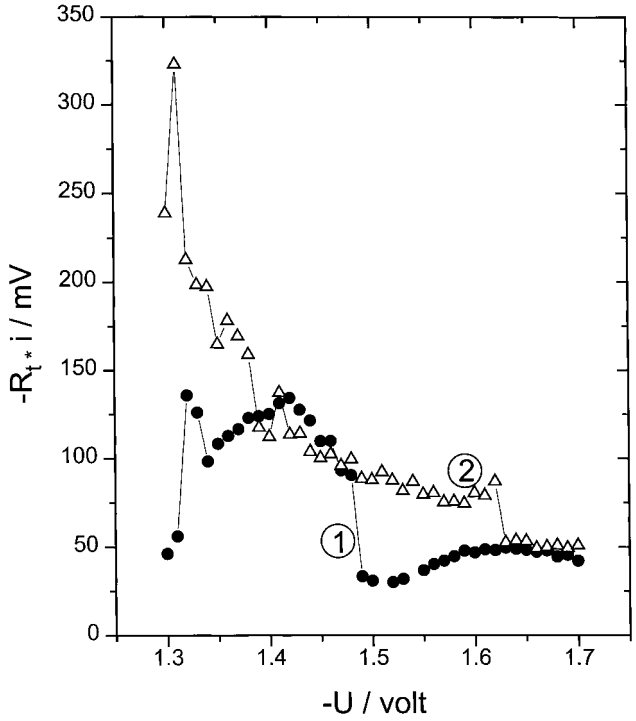

Fig. 13. Potential dependence of the $R_t i$ product under the same conditions as for Fig. 9; without Co^{2+} (curve 1) and with 100 mg dm^{-3} Co^{2+} (curve 2).

sorbed cobalt is characterized by relatively high values of the product of the charge transfer resistance, R_t, and current density, i, and also by relatively low values of the double layer capacitance consequent on the hydrogen adsorption.

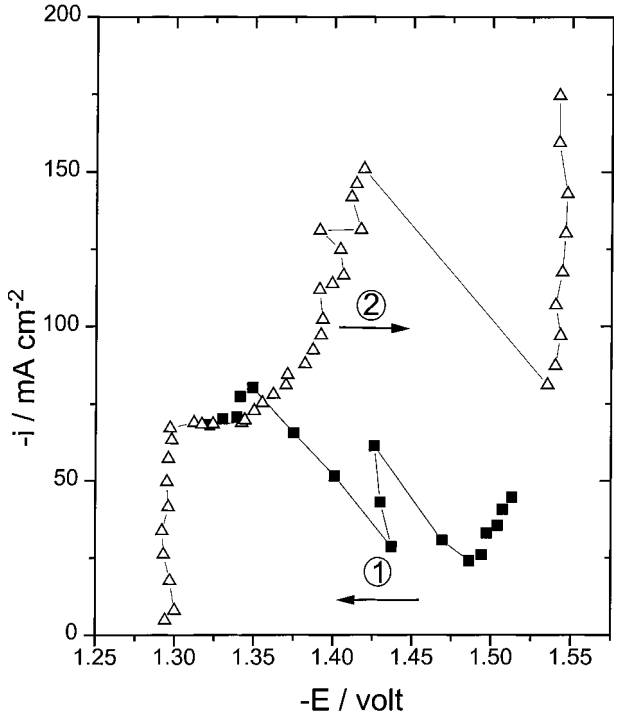

Fig. 14. Influence of the direction of potential stepping (indicated by arrows on the polarization curve). Aged electrolyte with [Co^{2+}] = 100 mg dm^{-3}. Curve 1: τ_p = 30 min at U = −1.56 V, then stepping U from −1.56 to −1.4 V. Curve 2: τ_p = 30 min at U = −1.3 V then stepping U from −1.3 to −1.7 V.

The influence of the electrolyte ageing indicates that the stimulation of hydrogen evolution by Co^{2+} ions occurs in combination with the catalytic effect of anodically formed products, as already reported for the nickel impurity. Adsorbed species originating from the anodic products progressively accumulate on the electrode surface and interfere with adsorbed cobalt to stimulate hydrogen evolution.

The stimulation of hydrogen evolution by cobalt adsorbed on zinc is accompanied by a redissolution of the zinc deposit, clearly detected from the potential dependencies of the current and double layer capacitance.

From the polarization curves, it is confirmed that hydrogen evolution on the zinc deposit is less sensitive to Co^{2+} ions than to Ni^{2+} ions.

Hydrogen evolution on the aluminium substrate is also stimulated by both adsorbed cobalt and anodically formed products. This reaction is inhibited in the presence of lead on the aluminium surface.

Acknowledgement

The authors acknowledge the financial help from the cooperation CNRS–Bulgarian Academy of Sciences (Project 2943), and from the Ministère de la Recherche et de la Technologie for a fellowship to Ts. Dobrev.

References

[1] M. Maja and P. Spinelli, *J. Electrochem. Soc.* **118** (1971) 1538.
[2] Y. Umetsu and K. Tozawa, *J. Mining Minerals Process. Inst., Jpn* **102** (1986) 429.

[3] D. R. Fosnacht and T. J. O'Keefe, *J. Appl. Electrochem.* **10** (1980) 495.
[4] M. Maja, N. Penazzi, R. Fratesi and G. Roventi, J. Electrochem. Soc., **129** (1982) 2695.
[5] S. Oyama and K. Taniuchi, *J. Mining Minerals Process. Inst.*, Jpn **90** (1974) 781.
[6] A. R. Ault and E. J. Frazer, *J. Appl. Electrochem.* **18** (1988) 583.
[7] E. J. Frazer, *J. Electrochem. Soc.* **135** (1988) 2465.
[8] C. Bozhkov, M. Petrova and St. Rashkov, *J. Appl. Electrochem.* **20** (1990) 17.
[9] D. J. Mackinnon, J. M. Brannen and P. L. Fenn, *ibid.* **17** (1987) 1129.
[10] R. Wiart, C. Cachet, Chr. Bozhkov and St. Rashkov, *ibid.* **20** (1990) 381.
[11] C. Cachet, R. Wiart, I. Ivanov and St. Rashkov, *ibid.* **23** (1993) 1011.
[12] D. R. Fosnacht and T. J. O'Keefe, *Metall. Trans. B* **14B** (1983) 645.
[13] Y. M. Wang, T. J. O'Keefe and W. J. James, *J. Electrochem. Soc.* **127** (1980) 2589.
[14] D. J. Mackinnon, R. M. Morrison and J. M. Brannen, *J. Appl. Electrochem.* **16** (1986) 53.
[15] Chr. Bozhkov, M. Petrova and St. Raskhov, *ibid.* **22** (1992) 73.
[16] C. Cachet and R. Wiart, *ibid.* **20** (1990) 1009.
[17] *Idem*, *J. Electrochem. Soc.* **141** (1994) 131.
[18] R. Ichino, C. Cachet and R. Wiart, *J. Appl. Electrochem.* **25** (1995) 556.
[19] *Idem*, *Electrochim. Acta* **41** (1996) 1031.
[20] C. Cachet, R. Ichino and R. Wiart, Proceedings of the 4th International Symposium on Electrochemistry in Mineral and Metal Processing, Los Angeles, 1996, edited by R. Woods, F. M. Doyle and P. Richardson, The Electrochemical Society, Pennington, NJ, Vol. **96**-6, p. 391.